

Analysis of hadronic decays of ψ/J particles in generalized Veneziano models.

II. The $\psi \rightarrow 3\pi$ decay

Jiro Kodaira

Department of Physics, Kyoto University, Kyoto, Japan

Ken Sasaki

Department of Physics, Yokohama National University, Yokohama, Japan

(Received 23 November 1977)

Constructing the amplitude for the $\psi \rightarrow 3\pi$ decay from the five-point Veneziano function for $K\bar{K} \rightarrow 3\pi$, we calculate the 3π Dalitz-plot density. This amplitude well explains the characteristic features of the experimental data. Calculation is also made with the Virasoro amplitude for the process $\psi \rightarrow 3\pi$ which was proposed by Cohen-Tannoudji *et al.* The Virasoro amplitude predicts an enhancement in the central region of the 3π Dalitz plot. This fact is in disagreement with the experimental plot. Ratios among relevant coupling constants and partial decay widths are evaluated with both our Veneziano amplitude and the Virasoro amplitude. Experimental data prefers our Veneziano amplitude for $\psi \rightarrow 3\pi$.

In our previous paper¹ (referred to hereafter as I), we suggested a mechanism which governs the hadronic decay of the ψ/J particle into ordinary hadrons, and studied, as a first application, the $\psi \rightarrow 3\pi$ decay channel.² We assumed that the ψ decays into ordinary hadrons through mixing with daughters of the ω and/or ϕ recurrences. In the case of the $\psi \rightarrow 3\pi$ decay, the daughters of the ω recurrence $\omega_{i=9}$, with mass of α_{ω}^{-1} ($i=9$), dominantly contribute. Hence, we could construct the amplitude $A(\psi \rightarrow 3\pi)$ for the process $\psi \rightarrow 3\pi$ from the five-point Veneziano amplitude for $K\bar{K} \rightarrow 3\pi$. Then, evaluating the relative strength of the coupling constants at the $\psi\rho\pi$, $\psi\rho'_f\pi$, $\psi g\pi$, and $\psi\rho'_g\pi$ vertices, we found that our amplitude $A(\psi \rightarrow 3\pi)$ well describes the gross features of the experimental data.

In this paper, we introduce the imaginary part into the ρ trajectory $\alpha_{\rho}(s)$ and calculate the Dalitz-plot density for $\psi \rightarrow 3\pi$. Agreement with the experimental 3π Dalitz plot is fairly good.

There is another work besides ours on the study of the $\psi \rightarrow 3\pi$ decays. Cohen-Tannoudji *et al.*³ proposed to use a Virasoro amplitude.⁴ Using this amplitude, we calculate the Dalitz-plot density and also the relative strength of various coupling constants. Comparison is made with our results. We find that the Virasoro amplitude predicts an enhancement in the central region [$\alpha(s) \approx \alpha(t) \approx 3$] of the 3π Dalitz plot, which is in disagreement with the experimental data.

We start with the $I=0$ part of the five-point Veneziano amplitude for $K\bar{K} \rightarrow 3\pi$, Eq. (2.8) in I,⁵

$$A^{I=0}(K\bar{K} \rightarrow 3\pi) \propto \epsilon_{\mu_1\mu_2\mu_3\mu_4} P_1^{\mu_1} P_2^{\mu_2} P_3^{\mu_3} P_4^{\mu_4} \sum_{P(3,4,5)} B_5(\alpha_{12}^{\omega} - 1, \alpha_{23}^{K^*} - 1, \alpha_{34}^{\rho} - 1, \alpha_{45}^{\rho} - 1, \alpha_{51}^{K^*} - 1), \tag{1}$$

where the function B_5 is defined as

$$B_5(\alpha_{12} - 1, \alpha_{23} - 1, \alpha_{34} - 1, \alpha_{45} - 1, \alpha_{51} - 1) = \int_0^1 du_1 du_4 u_1^{-\alpha_{12}} (1-u_1)^{-\alpha_{23}} u_4^{-\alpha_{45}} (1-u_4)^{-\alpha_{34}} (1-u_1 u_4)^{-\alpha_{51} + \alpha_{23} + \alpha_{34} - 1}.$$

We obtain the desired amplitude $A(\psi \rightarrow 3\pi)$ by evaluating the pole residue of Eq. (1) at $\alpha_{12}=9$, since $\alpha_{12}^{\omega}(m_{\psi}^2) \approx 9$, projecting out the $J=1$ part, and finally by factorizing the $K\bar{K}\omega_{i=9}$ vertex. (In general the daughter $\omega_{i=9}$ may be degenerate and the factorization does not hold. Here we have made a purely phenomenological assumption that only one state among the degenerate states $\omega_{i=9}$ dominantly couples to ψ and also to the $K\bar{K}$ channel, so that the factorization procedure is permitted.)

The final expression of our amplitude for $\psi \rightarrow 3\pi$ is [see Eq. (2.13) in I]

$$A(\psi \rightarrow 3\pi) = C \epsilon_{\mu\nu\sigma\lambda} P_3^{\mu} P_4^{\nu} P_5^{\sigma} e^{\lambda} \times [D(s, t, u) + D(t, u, s) + D(u, s, t)], \tag{2}$$

where e is the polarization vector of ψ , C is a normalization constant, and

$$\begin{aligned} s &= s_{34} = (P_3 + P_4)^2, \\ t &= s_{45} = (P_4 + P_5)^2, \\ u &= s_{53} = (P_5 + P_3)^2. \end{aligned}$$

The scalar amplitude $D(s, t, u)$ has the following form:

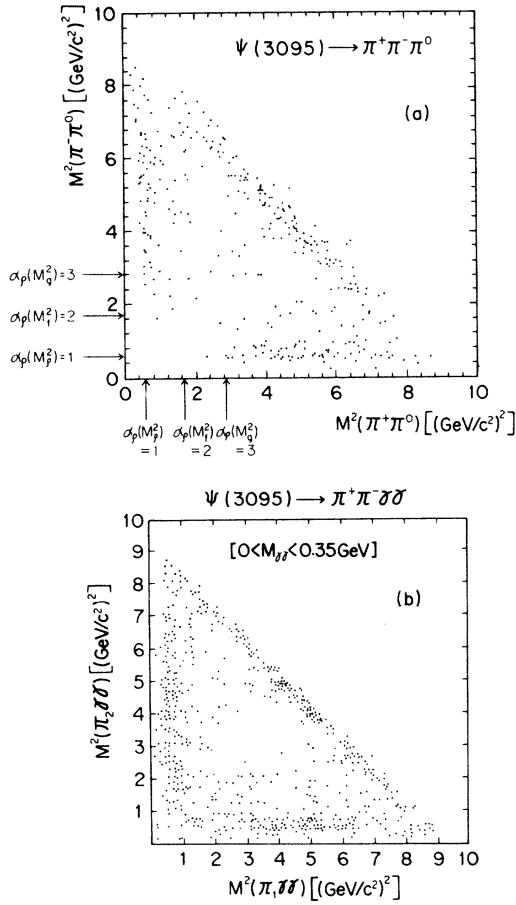


FIG. 1. (a) Experimental 3π Dalitz plot from B. Jean-Marie *et al.* (Ref. 2). (b) Dalitz plot for events fulfilling the condition that the invariant mass $m_{\gamma\gamma}$ in the $\psi \rightarrow \pi^+\pi^-\gamma\gamma$ decay channel is confined to the π^0 interval ($0 < m_{\gamma\gamma} < 0.35$ GeV/c²). See W. Bartel *et al.* (Ref. 2).

$$D(s, t, u) = \sum_{n=1}^9 C_n(s, t, u) B(n - \alpha_\rho(s), 1 - \alpha_\rho(t)). \quad (3)$$

Other amplitudes, $D(t, u, s)$ and $D(u, s, t)$, are obtained from Eq. (3) by cyclic permutation. The coefficients $C_n(s, t, u)$ are polynomials in the variables s , t , and u , and their explicit expressions are shown in the Appendix. The pole structures arise from the Euler beta functions B .

The term $D(s, t, u)$ in Eq. (2) comes from the sum of particular particle configurations (3, 4, 5) and (5, 4, 3), so the relation

$$D(s, t, u) = D(t, s, u)$$

holds. Similarly, we have

$$D(t, u, s) = D(u, t, s), \quad D(u, s, t) = D(s, u, t).$$

$$V(s, t, u) = \beta \frac{\Gamma(\frac{1}{2} - \frac{1}{2}\alpha(s))\Gamma(\frac{1}{2} - \frac{1}{2}\alpha(t))\Gamma(\frac{1}{2} - \frac{1}{2}\alpha(u))}{\Gamma(1 - \frac{1}{2}\alpha(s) - \frac{1}{2}\alpha(t))\Gamma(1 - \frac{1}{2}\alpha(t) - \frac{1}{2}\alpha(u))\Gamma(1 - \frac{1}{2}\alpha(u) - \frac{1}{2}\alpha(s))}. \quad (8)$$

Therefore our amplitude, Eq. (2), is symmetric in the variables s , t , and u . Also, it has an interesting property which was emphasized in I: residues at even poles turn out to be zero in the limit $m_\pi^2 = 0$.

Next, we calculate the Dalitz-plot density. First, we introduce the imaginary part into the ρ trajectory $\alpha_\rho(s)$. The ρ signals are clearly seen in the experimental data² in Fig. 1. Thus we choose the imaginary part so as to reproduce the ρ width. Since the ρ width is about 0.15 GeV, we take

$$\alpha_\rho(s) = 0.48 + 0.89s + i0.14(s - 4m_\pi^2)^{1/2}. \quad (4)$$

Now that the trajectory $\alpha_\rho(s)$ has an imaginary part, the expression of Eq. (2) becomes asymmetric in the variables s , t , and u . So we rewrite Eq. (2) such that the amplitude is manifestly symmetric in s , t , and u ,

$$\begin{aligned} \tilde{A}(\psi \rightarrow 3\pi) = \frac{1}{2} C \epsilon_{\mu\nu\sigma\lambda} P_3^\mu P_4^\nu P_5^\sigma e^{\lambda\rho} [& D(s, t, u) + D(t, s, u) \\ & + D(t, u, s) + D(u, t, s) \\ & + D(u, s, t) + D(s, u, t)]. \end{aligned} \quad (5)$$

The Dalitz-plot density for the final three pions should be proportional to

$$|\tilde{A}(\psi \rightarrow 3\pi)|^2.$$

The resulting Dalitz plot is shown in Fig. 2. Comparing that with the experimental plots in Figs. 1(a) and 1(b), we find that the agreement is fairly good. Especially, we can explain the experimental fact in the $\psi \rightarrow 3\pi$ decays that the $\rho\pi$ channel is dominant. We should note that the kinematical factor in Eq. (5) has the effect of enhancing the central region, because

$$\sum_{\text{spin}} |\epsilon_{\mu\nu\sigma\lambda} P_3^\mu P_4^\nu P_5^\sigma e^{\lambda\rho}|^2 = \frac{1}{4} [stu - m_\pi^2(m_\psi^2 - m_\pi^2)^2]. \quad (6)$$

But the sum of the scalar amplitude $D(s, t, u)$ and others surpasses the effect of the kinematical factor and gives rise to suppression in the central region of the Dalitz plot.

A different idea from ours on the decay of $\psi \rightarrow 3\pi$ is proposed by Cohen-Tannoudji *et al.*³ They pointed out that the following Virasoro amplitude⁴ should be used for the reaction $\psi \rightarrow \pi(P_3) + \pi(P_4) + \pi(P_5)$:

$$A(s, t, u) = \epsilon_{\mu\nu\sigma\lambda} P_3^\mu P_4^\nu P_5^\sigma e^{\lambda V}(s, t, u), \quad (7)$$

where

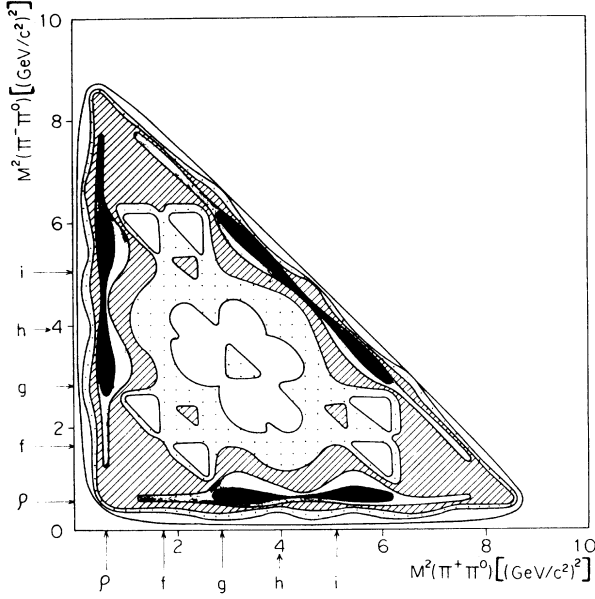


FIG. 2. Predictions of our Veneziano model for the 3π Dalitz plot. The diagram is divided into four parts according to the density of events (maximum = 10) as follows: \square 0–0.01 \textbackslash 0.1–0.5 \textbackslash 0.5–2.5 \blacksquare 2.5–6 \bullet 6–10.

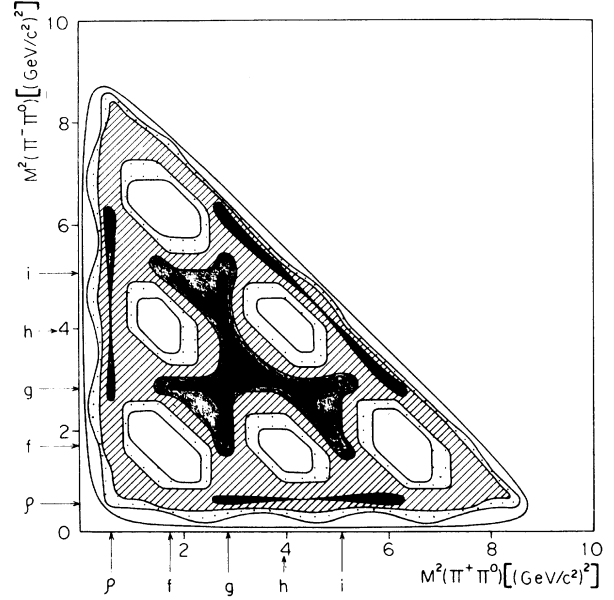


FIG. 3. Predictions of the Virasoro model.

This Virasoro amplitude does not have poles at even integers of α_ρ .

Using Eqs. (7) and (8) and the α_ρ in Eq. (4), we can calculate the Dalitz-plot density. The result is shown in Fig. 3. Unlike our Veneziano model for $\psi \rightarrow 3\pi$, we find an enhancement in the central region of the 3π Dalitz plot. This disagrees with the features of the experimental 3π plot.

In order to study the origin of the enhancement more closely, we evaluate the Virasoro amplitude at the poles of $\alpha(s)=1, 3$, and 5 , which correspond to the poles of the recurrences $\rho(1^-)$, $g(3^-)$, and $i(5^-)$, respectively.⁶ Then we calculate the relative strength of the various coupling constants. We define the coupling constants as follows⁷:

$$f_{\psi\rho\pi} \in \mu\nu\lambda\sigma (\partial^\mu \psi^\nu) (\partial^\lambda \rho_i^\sigma) \pi_i, \quad (9)$$

$$\frac{1}{8} f_{\psi g\pi} \in \mu\nu\lambda\sigma (\pi_i \bar{\partial}_\kappa \bar{\partial}_\tau \bar{\partial}_\lambda \psi^\nu) (\partial^\sigma g_i^{\mu\kappa\tau}), \quad (10)$$

$$\frac{1}{32} f_{\psi i\pi} \in \mu\nu\lambda\sigma (\pi_i \bar{\partial}_{\alpha_2} \cdots \bar{\partial}_{\alpha_5} \bar{\partial}_\lambda \psi^\nu) (\partial^{\sigma i\mu} \alpha_2 \cdots \alpha_5), \quad (11)$$

$$\frac{1}{2} f_{\rho\pi\pi} \in ijk (\pi_i \bar{\partial}_\mu \pi_j) \rho_k^\mu, \quad (12)$$

$$\frac{1}{8} f_{g\pi\pi} \in ijk (\pi_i \bar{\partial}_\mu \bar{\partial}_\nu \bar{\partial}_\lambda \pi_j) g_k^{\mu\nu\lambda}, \quad (13)$$

$$\frac{1}{32} f_{i\pi\pi} \in ijk (\pi_i \bar{\partial}_{\alpha_1} \cdots \bar{\partial}_{\alpha_5} \pi_j) i_k^{\alpha_1 \cdots \alpha_5}. \quad (14)$$

Other coupling constants related to the daughter particles $\rho'_g(1^-)$, $\rho'_i(1^-)$, and $g'_i(3^-)$ have forms similar to Eqs. (9), (10), (12), and (13).

Calculations have been done in the limit $m_\pi^2=0$, i.e., $\alpha_\rho(0)=\frac{1}{2}$, and we arrive at the following ratios:

TABLE I. The relative strength of the various coupling constants in the Virasoro and the Veneziano models. The normalizations of the f 's are defined in the text.

	$f_{\psi g\pi}^2 / f_{\psi\rho\pi}^2$ [(GeV/c ²) ⁻⁴]	$f_{\psi\rho'_g\pi}^2 / f_{\psi\rho\pi}^2$	$f_{\psi i\pi}^2 / f_{\psi\rho\pi}^2$ [(GeV/c ²) ⁻⁸]	$f_{\psi g'_i\pi}^2 / f_{\psi\rho\pi}^2$ [(GeV/c ²) ⁻⁴]	$f_{\psi\rho'_i\pi}^2 / f_{\psi\rho\pi}^2$
Virasoro model	3.2×10^{-2}	2.8×10^1	3.1×10^{-3}	1.2	4.5×10^1
Veneziano model	7.4×10^{-2}	5.9×10^{-1}	4.6	4.1	6.7×10^{-1}

TABLE II. The ratios of the partial decay widths of ψ in the Virasoro and the Veneziano models.

	$\frac{\Gamma(\psi \rightarrow g\pi)}{\Gamma(\psi \rightarrow \rho\pi)}$	$\frac{\Gamma(\psi \rightarrow \rho'_g\pi)}{\Gamma(\psi \rightarrow \rho\pi)}$	$\frac{\Gamma(\psi \rightarrow i\pi)}{\Gamma(\psi \rightarrow \rho\pi)}$	$\frac{\Gamma(\psi \rightarrow g'_i\pi)}{\Gamma(\psi \rightarrow \rho\pi)}$	$\frac{\Gamma(\psi \rightarrow \rho'_i\pi)}{\Gamma(\psi \rightarrow \rho\pi)}$
Virasoro model	6.0×10^{-2}	12	2.9×10^{-5}	4.1×10^{-2}	5.6
Veneziano model	1.4×10^{-1}	2.5×10^{-1}	4.3×10^{-2}	1.4×10^{-1}	8.3×10^{-2}

$$f_{\psi\rho\pi}^2 f_{\rho\pi\pi}^2 : f_{\psi g\pi}^2 f_{g\pi\pi}^2 : f_{\psi\rho'_g\pi}^2 f_{\rho'_g\pi\pi}^2 : f_{\psi i\pi}^2 f_{i\pi\pi}^2 : f_{\psi g'_i\pi}^2 f_{g'_i\pi\pi}^2 : f_{\psi\rho'_i\pi}^2 f_{\rho'_i\pi\pi}^2$$

$$= 1 : 5.1 \times 10^{-2} (\text{GeV}/c^2)^{-8} : 1.7 : 1.3 \times 10^{-3} (\text{GeV}/c^2)^{-16} : 2.0 \times 10^{-1} (\text{GeV}/c^2)^{-8} : 1.5. \quad (15)$$

Note that the Virasoro amplitude predicts the coupling strength of $f_{\psi\rho'_g\pi}^2 f_{\rho'_g\pi\pi}^2$ to be roughly twice as large as that of $f_{\psi\rho\pi}^2 f_{\rho\pi\pi}^2$. This fact and the kinematical factor in Eq. (7) join together to produce the enhancement in the central region of the 3π plot.

Further, the ratios of $f_{g\pi\pi}^2/f_{\rho\pi\pi}^2$, $f_{i\pi\pi}^2/f_{\rho\pi\pi}^2$, and others can be obtained from the Veneziano amplitude for the $\pi\pi$ elastic amplitude with the $I=1$ state in the s channel,⁸ Eq. (3.10) in I. They are (in the limit $m_\pi^2=0$)

$$\frac{f_{i\pi\pi}^2}{f_{\rho\pi\pi}^2} = \frac{2}{3} \alpha'^4, \quad \frac{f_{g'_i\pi\pi}^2}{f_{\rho\pi\pi}^2} = \frac{5}{24} \alpha'^2, \quad \frac{f_{\rho'_i\pi\pi}^2}{f_{\rho\pi\pi}^2} = \frac{29}{896},$$

$$\frac{f_{g\pi\pi}^2}{f_{\rho\pi\pi}^2} = 2 \alpha'^2, \quad \frac{f_{\rho'_g\pi\pi}^2}{f_{\rho\pi\pi}^2} = \frac{1}{16}.$$

Using these values, we obtain the ratios of relevant coupling constants to $f_{\psi\rho\pi}^2$. They are listed in Table I. Also listed are the predicted values for the same quantities in our Veneziano model.

Finally, we calculate the ratios of the partial decay widths of ψ into $g\pi$, $i\pi$, etc., to that of ψ into $\rho\pi$ both in the Virasoro and the Veneziano models. They are listed in Table II. From Table II, we see that the Virasoro model predicts very large values for the partial decay widths of ψ into $\rho'_g\pi$ and $\rho'_i\pi$.

Why does our Veneziano model for $\psi \rightarrow 3\pi$ give

rise to suppression in the central region of the 3π Dalitz plot? This may have some relation to the fact that the dual resonance model (more precisely a six-point Veneziano function) predicts the exponential damping at large transverse momentum in the single-particle inclusive spectra of hadron-hadron scatterings.⁹ Indeed there is a difference between decay and scattering processes in the respect of the physical regions of the Mandelstam diagram. But both the central part in the $\psi \rightarrow 3\pi$ Dalitz plot and the kinematical region in the large-transverse-momentum phenomena correspond to where $|s|$, $|t|$, and $|u|$ are large. In this respect, it may be very probable that there are close connections between the predicted features of the two phenomena by the dual resonance model.

ACKNOWLEDGMENT

We would like to thank Professor M. Ida, Professor T. Muta, Dr. M. Bando, Dr. S. Kitakado, Dr. H. Yabuki, Dr. M. Kobayashi, Dr. S. Yazaki, and Dr. T. Uematsu for many important suggestions, valuable comments, and discussions throughout the preparation of this work. We also thank Professor M. Ida for reading the manuscript. One of us (K. S.) would like to thank Professor H. Sato for the hospitality extended to him at the Research Institute for Fundamental Physics where part of this work was done.

APPENDIX

In this appendix the explicit forms of the $C_n(s, t, u)$ in Eq. (3) are presented. The functions a_s , b_u , g_s , g_u , and $h_{s,u}$ are defined as follows:

$$a_s = \frac{1}{2} (\alpha_{25}^{K^*} + \alpha_{15}^{K^*}) = \frac{1}{2} (\alpha' s - \frac{15}{2}),$$

$$b_u = \frac{1}{2} (\alpha_{31}^{K^*} - \alpha_{25}^{K^*} - \alpha_{45}^{\rho} + 1 + \alpha_{23}^{K^*} - \alpha_{15}^{K^*} - \alpha_{45}^{\rho} + 1) = \frac{1}{2} [\alpha' u + 2\alpha_{\rho}(0) - \frac{17}{2}],$$

$$g_s = \frac{9 - \alpha_{\rho}(0) - 4[\frac{1}{2} - \alpha_{K^*}(0)]}{4[9 - \alpha_{\rho}(0)]} \{ [\alpha' s + 2\alpha_{\rho}(0) - \frac{19}{2}]^2 - 2[9 - \alpha_{\rho}(0)][1 - 2\alpha_{\rho}(0)] \},$$

$$g_u = \frac{9 - \alpha_\rho(0) - 4[\frac{1}{2} - \alpha_{K^*}(0)]}{4[9 - \alpha_\rho(0)]} \{[\alpha'u + 2\alpha_\rho(0) - \frac{19}{2}]^2 - 2[9 - \alpha_\rho(0)][1 - 2\alpha_\rho(0)]\},$$

$$h_{s,u} = \frac{9 - \alpha_\rho(0) - 4[\frac{1}{2} - \alpha_{K^*}(0)]}{4[9 - \alpha_\rho(0)]} \{[\alpha's + \frac{17}{2}][\alpha'u + \frac{17}{2}] - 17[9 - \alpha_\rho(0)]\},$$

where α' is the universal trajectory slope ($=0.89 \text{ GeV}^{-2}$).

$$C_1(s, t, u) = \binom{8}{0} [2a_s(a_s + 1) \cdots (a_s + 7) + \frac{4}{5}g_s(14a_s^6 + 294a_s^5 + 2415a_s^4 + 9800a_s^3 + 20307a_s^2 + 19698a_s + 6534)$$

$$+ \frac{6}{5}g_s^2(10a_s^4 + 140a_s^3 + 690a_s^2 + 1400a_s + 967) + \frac{4}{3}g_s^3(2a_s^2 + 14a_s + 23) + \frac{2}{33}g_s^4],$$

$$C_2(s, t, u) = \binom{8}{1} \{b_u[2a_s(a_s + 1) \cdots (a_s + 6) + \frac{14}{5}g_s(a_s + 3)(3a_s^4 + 36a_s^3 + 142a_s^2 + 204a_s + 84)$$

$$+ 6g_s^2(a_s + 3)(a_s^2 + 6a_s + 7) + \frac{2}{3}g_s^3(a_s + 3)]$$

$$+ h_{s,u}[\frac{6}{5}(7a_s^6 + 126a_s^5 + 875a_s^4 + 2940a_s^3 + 4872a_s^2 + 3528a_s + 720)$$

$$+ \frac{6}{5}g_s(5a_s^4 + 60a_s^3 + 250a_s^2 + 420a_s + 232) + \frac{2}{3}g_s^2(3a_s^2 + 18a_s + 25) + \frac{2}{33}g_s^3]\},$$

$$C_3(s, t, u) = \binom{8}{2} \{b_u(b_u + 1)[2a_s \cdots (a_s + 5) + \frac{2}{5}g_s(15a_s^4 + 150a_s^3 + 510a_s^2 + 675a_s + 274) + \frac{6}{7}g_s^2(3a_s^2 + 15a_s + 17) + \frac{2}{21}g_s^3]$$

$$+ g_u[\frac{2}{5}a_s(a_s + 1) \cdots (a_s + 5) + \frac{2}{35}g_s(15a_s^4 + 150a_s^3 + 510a_s^2 + 675a_s + 274) + \frac{2}{21}g_s^2(3a_s^2 + 15a_s + 17) + \frac{2}{231}g_s^3]$$

$$+ (2b_u + 1)h_{s,u}[\frac{2}{5}(2a_s + 5)(3a_s^4 + 30a_s^3 + 95a_s^2 + 100a_s + 24) + \frac{6}{7}g_s(2a_s + 5)(2a_s^2 + 10a_s + 9) + \frac{2}{7}g_s^2(2a_s + 5)]$$

$$+ h_{s,u}^2[\frac{4}{35}(15a_s^4 + 150a_s^3 + 510a_s^2 + 675a_s + 274) + \frac{8}{21}g_s(3a_s^2 + 15a_s + 17) + \frac{4}{77}g_s^2]\},$$

$$C_4(s, t, u) = \binom{8}{3} \{b_u(b_u + 1)(b_u + 2)[2a_s(a_s + 1) \cdots (a_s + 4) + 2g_s(a_s + 2)(2a_s^2 + 8a_s + 5) + \frac{6}{7}g_s^2(a_s + 2)]$$

$$+ 3g_u(b_u + 1)[\frac{2}{5}a_s(a_s + 1) \cdots (a_s + 4) + \frac{2}{7}g_s(a_s + 2)(2a_s^2 + 8a_s + 5) + \frac{2}{21}g_s^2(a_s + 2)]$$

$$+ h_{s,u}(3b_u^2 + 6b_u + 2)[\frac{2}{5}(5a_s^4 + 40a_s^3 + 105a_s^2 + 100a_s + 24) + \frac{6}{7}g_s(2a_s^2 + 8a_s + 7) + \frac{2}{21}g_s^2]$$

$$+ \frac{6}{7}h_{s,u}g_u[\frac{1}{5}(5a_s^4 + 40a_s^3 + 105a_s^2 + 100a_s + 24) + \frac{1}{3}g_s(2a_s^2 + 8a_s + 7) + \frac{1}{33}g_s^2]$$

$$+ 3h_{s,u}^2(b_u + 1)[\frac{4}{7}(a_s + 2)(2a_s^2 + 8a_s + 5) + \frac{8}{21}g_s(a_s + 2)] + h_{s,u}^3[\frac{4}{21}(2a_s^2 + 8a_s + 7) + \frac{8}{231}g_s]\},$$

$$C_5(s, t, u) = \binom{8}{4} \{2b_u(b_u + 1) \cdots (b_u + 3)[a_s \cdots (a_s + 3) + \frac{1}{5}g_s(6a_s^2 + 18a_s + 11) + \frac{3}{35}g_s^2]$$

$$+ 2g_u(6b_u^2 + 18b_u + 11)[\frac{1}{5}a_s \cdots (a_s + 3) + \frac{1}{35}g_s(6a_s^2 + 18a_s + 11) + \frac{1}{105}g_s^2]$$

$$+ \frac{2}{35}g_u^2[3a_s \cdots (a_s + 3) + \frac{1}{3}g_s(6a_s^2 + 18a_s + 11) + \frac{1}{11}g_s^2]$$

$$+ 8h_{s,u}(2b_u + 3)(b_u^2 + 3b_u + 1)[\frac{1}{5}(2a_s + 3)(a_s^2 + 3a_s + 1) + \frac{3}{35}g_s(2a_s + 3)]$$

$$+ 8h_{s,u}g_u(2b_u + 3)[\frac{3}{35}(2a_s + 3)(a_s^2 + 3a_s + 1) + \frac{1}{35}g_s(2a_s + 3)]$$

$$+ 2h_{s,u}^2(6b_u^2 + 18b_u + 11)[\frac{2}{35}(6a_s^2 + 18a_s + 11) + \frac{4}{105}g_s] + \frac{2}{35}h_{s,u}^2g_u[\frac{4}{3}(6a_s^2 + 18a_s + 11) + \frac{8}{11}g_s]$$

$$+ \frac{16}{105}h_{s,u}^3(2b_u + 3)(2a_s + 3) + \frac{2}{35} \times \frac{8}{33}h_{s,u}^4\}.$$

Four other coefficients, $C_6(s, t, u)$, $C_7(s, t, u)$, $C_8(s, t, u)$, and $C_9(s, t, u)$, are obtained by interchanging a_s with b_u , and g_s with g_u , in the expressions of $C_4(s, t, u)$, $C_3(s, t, u)$, $C_2(s, t, u)$, and $C_1(s, t, u)$, respectively.

¹J. Kodaira and K. Sasaki, Phys. Rev. D **17**, 1381 (1978).

²B. Jean-Marie *et al.*, Phys. Rev. Lett. **36**, 291 (1976);

W. Bartel *et al.*, Phys. Lett. **64B**, 483 (1976).

³G. Cohen-Tannoudji *et al.*, Phys. Lett. **62B**, 343 (1976).

⁴M. A. Virasoro, Phys. Rev. **177**, 2309 (1969).

⁵K. Bardakci and H. Ruegg, Phys. Lett. **28B**, 671 (1969).

⁶Calculations had already been done by Z. Z. Aydin.

But he did not obtain the values of coupling constants for $\psi\rho'_s\pi$, $\psi\rho'_i\pi$, and $\psi g'_i\pi$ vertices; Z. Z. Aydin, Lett. Nuovo Cimento **19**, 573 (1977).

⁷M. D. Scadron, Phys. Rev. **165**, 1640 (1968).

⁸C. Lovelace, Phys. Lett. **28B**, 264 (1968).

⁹This remark was first pointed out to the authors by S. Yazaki.

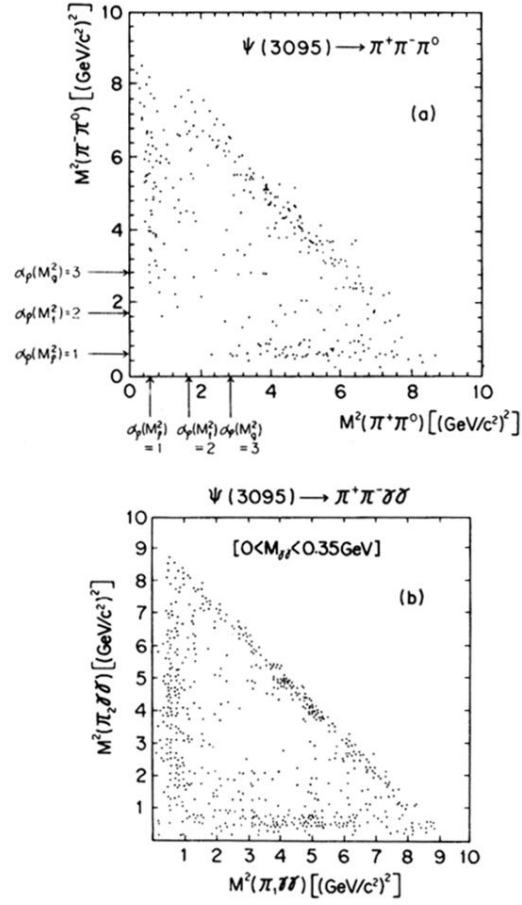


FIG. 1. (a) Experimental 3π Dalitz plot from B. Jean-Marie *et al.* (Ref. 2). (b) Dalitz plot for events fulfilling the condition that the invariant mass $m_{\gamma\gamma}$ in the $\psi \rightarrow \pi^+\pi^-\gamma\gamma$ decay channel is confined to the π^0 interval ($0 < m_{\gamma\gamma} < 0.35 \text{ GeV}/c^2$). See W. Bartel *et al.* (Ref. 2).

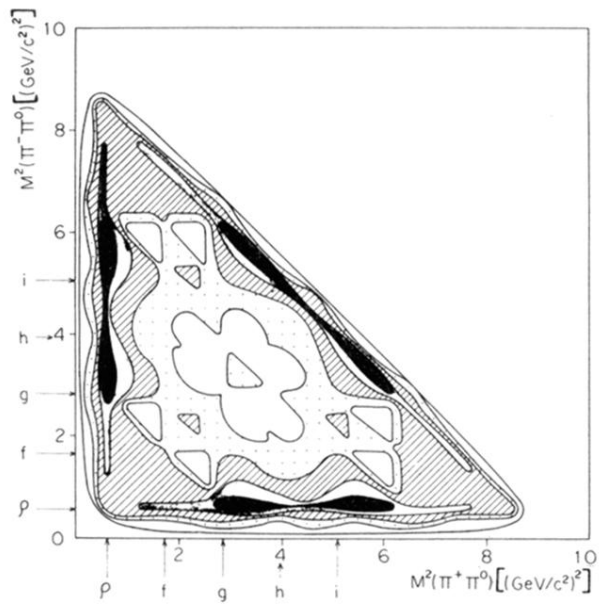


FIG. 2. Predictions of our Veneziano model for the 3π Dalitz plot. The diagram is divided into four parts according to the density of events (maximum = 10) as follows: \square 0–0.01 \boxtimes 0.1–0.5 \boxdot 0.5–2.5 \blacksquare 2.5–6 \blacksquare 6–10.

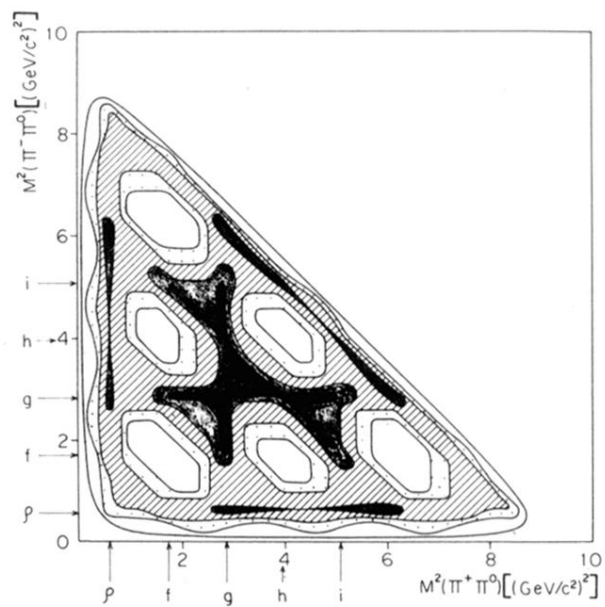


FIG. 3. Predictions of the Virasoro model.